

# A highly sensitive search for magnetic fields in B, A and F stars<sup>★</sup>

S. L. S. Shorlin<sup>1</sup>, G. A. Wade<sup>2</sup>, J.-F. Donati<sup>3</sup>, J. D. Landstreet<sup>1,3</sup>, P. Petit<sup>3</sup>, T. A. A. Sigut<sup>1</sup>, and S. Strasser<sup>1,4</sup>

<sup>1</sup> Physics & Astronomy Department, The University of Western Ontario, London, Ontario, N6A 3K7 Canada

<sup>2</sup> Department of Physics, Royal Military College of Canada, Kingston, Ontario, K7K 7B4 Canada

<sup>3</sup> Observatoire Midi-Pyrénées, 14 Avenue Edouard Belin, 31400 Toulouse, France

<sup>4</sup> Physics and Astronomy Department, University of Calgary, Calgary, Alberta, T2N 1N4 Canada

Received 27 Mars 2002 / Accepted 20 June 2002

**Abstract.** Circular spectropolarimetric observations of 74 stars were obtained in an attempt to detect magnetic fields via the longitudinal Zeeman effect in their spectral lines. The sample observed includes 22 normal B, A and F stars, four emission-line B and A stars, 25 Am stars, 10 HgMn stars, two  $\lambda$  Boo stars and 11 magnetic Ap stars. Using the Least-Squares Deconvolution multi-line analysis approach (Donati et al. 1997), high precision Stokes  $I$  and  $V$  mean signatures were extracted from each spectrum. We find absolutely no evidence for magnetic fields in the normal, Am and HgMn stars, with upper limits on longitudinal field measurements usually considerably smaller than any previously obtained for these objects. We conclude that if any magnetic fields exist in the photospheres of these stars, these fields are not ordered as in the magnetic Ap stars, nor do they resemble the fields of active late-type stars. We also detect for the first time a field in the A2pSr star HD 108945 and make new precise measurements of longitudinal fields in five previously known magnetic Ap stars, but do not detect fields in five other stars classified as Ap SrCrEu. We also report new results for several binary systems, including a new  $v \sin i$  for the rapidly rotating secondary of the Am- $\delta$  Del SB2 HD 110951.

**Key words.** line: profiles – polarization – stars: chemically peculiar – stars: magnetic fields – stars: atmospheres

## 1. Introduction

Preston's (1974) classification of the chemically peculiar A and B type stars into magnetic and non-magnetic subtypes has generally been found to be valid. The existence of strong, ordered magnetic fields in many Ap SrCrEu, Ap Si, He-weak SiSrTi, and He-strong stars, and the lack of detectable fields among the Ap HgMn, Am, He-weak PGa and  $\lambda$  Boo stars (Conti 1969; Borra & Landstreet 1980; Landstreet 1982; Borra et al. 1983; Bohlender & Landstreet 1990) appears to be a real (and important) physical property distinguishing the two classes. This is strongly supported by the fact that neither the Am stars, the Ap HgMn stars, nor the He-weak PGa exhibit *any* of the phenomenology associated with magnetic stars on the upper (or the lower) main sequence. They do not show the photometric or line profile variability common among the magnetic upper main sequence stars (although isolated reports do exist; see for example Rao et al. 1990), nor do they exhibit the resonance line emission, X-ray emission, and photometric variability (attributed to spottedness) accepted as indicators of magnetism among the late-type stars.

Send offprint requests to: S. L. S. Shorlin,  
e-mail: sshorlin@astro.uwo.ca

<sup>★</sup> Based on observations obtained using the MuSiCoS spectropolarimeter on the Bernard Lyot telescope, l'Observatoire du Pic du Midi, France.

However, a number of studies published within the past decade indicate that perhaps the situation is not quite so clear-cut as was originally suggested. In particular, apparently significant detections of strong, complex magnetic fields in the Am stars  $\sigma$  Peg (HD 214994) (Mathys 1988; Mathys & Lanz 1990) and 15 Vul (HD 189849) (Bikmaev et al. 1998), and in the Ap HgMn stars  $\chi$  Lup (HD 141556) and 74 Aqr (HD 214694) (Mathys & Hubrig 1995) have been made using the apparent desaturation of lines with different magnetic sensitivities. Such detections suggest that magnetic fields may exist in at least *some* classical non-magnetic stars and are perhaps more like those of active FGKM stars than those of the well-known magnetic A and B stars. Furthermore, reported probable detections of magnetic fields in two of three Am stars studied by Lanz & Mathys (1993; HD 29173 and HD 195479A) may indicate that similar magnetic fields exist in *most* classical non-magnetic stars, or at least in the Am stars. Confirmation of this possibility would profoundly modify our understanding of stellar atmosphere physics in this area of the HR diagram. It would provide important new constraints on the mechanisms responsible for magnetism in the early-type stars, as well as on the physical processes responsible for the chemical peculiarities observed to some degree in almost *all* A-type stars.

Finally, in order to solve the problem of the origins of magnetic fields in the mid to upper-main sequence, one must understand what the problem really is. Do 5% of A stars have large-

scale ordered fields, as we have assumed in the past, while the others are non-magnetic, or do some or all of the others have magnetic fields, but magnetic fields which are of a different nature than those in the classical magnetic Ap stars? The two cases are very different, and one cannot expect to address the problem of field origins without determining which best describes the true situation. For all these reasons we have carried out a large programme to search for magnetic fields in all kinds of B, A, and F stars.

## 2. Detection of stellar magnetic fields

The classical method for detecting stellar magnetic fields in the mid to upper main sequence has been the detection of circular polarization in spectral lines due to the line-of-sight component of a star's magnetic field. The quantity inferred from spectropolarimetric observations is the line-intensity weighted average over the stellar disk of the line-of-sight component of the magnetic field, referred to as the longitudinal field or effective field. Stars which have detectable longitudinal magnetic fields exhibit the chemical peculiarities we now associate with magnetic Ap stars, and they nearly always exhibit photometric and/or line profile variation with the same period as the variation in longitudinal field. Stars which show chemical peculiarities typical of magnetic Ap stars and/or periodic photometric and line profile variations, but for which no longitudinal fields have been detected, are usually assumed to have fields smaller than the observational errors.

Conversely, no longitudinal magnetic fields have been convincingly detected for the non-Ap stars. The upper limits on longitudinal field strengths have typically been of the order of 100 G (Borra & Landstreet 1980). If recent observations of non-magnetic stars, implying mean field moduli of several kilogauss, are correct, then 100 G longitudinal fields do put some constraint on the complexity of the stars' global field structures. Improving the precision of longitudinal field measurement, however, could perhaps make possible the detection of a weak net longitudinal component, or more tightly constrain the topology of a possible complex field.

Since the complex magnetic fields reported may be similar to those observed in cool active stars, the use of a field detection method which works well for active stars is needed. To this end, we have employed the cross-correlation technique Least-Squares Deconvolution (LSD; Donati et al. 1997) to analyze circularly polarized spectra of non-magnetic stars mostly having significantly non-zero  $v \sin i$ . LSD takes advantage of the similar shapes of spectral lines and their associated polarization features in order to obtain large improvements in the signal-to-noise ratios ( $S/N$ ) of Stokes  $V$  profiles by using the information contained in all of the lines in the stellar spectrum. Donati et al. (1997) have employed LSD to detect the very weak circularly polarized (Stokes  $V$ ) signatures in the spectral lines of a number of active late-type stars. The disk-integrated magnetic field strength reported for  $\alpha$  Peg is of the order of that deduced by Donati (1999) for the active star HR 1099. We expect that this technique should therefore be very effective for detecting such complex fields. In Fig. 1 we show illustrative LSD mean unpolarized (Stokes  $I$ ) and Stokes  $V$  sig-

natures for the RS CVn binary HR 1099 (Donati 1999). The full amplitude of the Stokes  $V$  signal is about 0.1%, and it is clearly detected in the LSD spectrum which has a  $S/N$  of 9100:1. Zeeman-Doppler imaging of the parent magnetic field configuration (Donati 1999) shows that the Stokes  $V$  morphology and modulation of HR 1099 imply a very complex surface magnetic field with a brightness-weighted unsigned averaged longitudinal field strength over the surface of about 200 G.

Wade et al. (2000b) used LSD extracted Stokes  $V$  profiles to measure longitudinal fields of magnetic Ap stars, and typically improved the standard errors of field measurements by a factor of five to ten over previous work. This improvement in precision is expected to allow us to greatly improve on upper limits for longitudinal fields of the non-magnetic stars.

A strong motivation for this study is our concern that the methods which have been used recently to detect magnetic fields in the canonically non-magnetic chemically peculiar stars are ambiguous, since they employ the subtle effects of magnetic intensification in spectral lines (often a single pair of lines) as their magnetic diagnostic. As pointed out by Hubrig & Castelli (2001), uncertainties in atomic physics, as well as possible unrecognized blends, cause these methods of detection to be somewhat uncertain themselves. Although we are unable to use our observations to make similar measurements of mean field moduli for B, A, and F stars, we are able to provide very precise circular polarization profiles. The modelling of polarization profiles to constrain stellar magnetic field parameters, including field moduli, will be the subject of a future paper.

Another motivation for this study is as a test of the performance of the LSD technique at detecting magnetic fields in a varied population of stars. Previously, work with LSD has been concentrated on relatively well-studied magnetic Ap stars and on cool active stars. Our use of LSD for the study of magnetic fields in stars with a range of chemical peculiarities, rotation velocities, temperatures and gravities allows us to determine where our technique is most applicable, as well as where it may be limited.

## 3. Observations

Stokes  $V$  and Stokes  $I$  spectra of 25 Am stars, 10 HgMn stars, two  $\lambda$  Boo stars, 22 normal stars, 11 stars of "magnetic" Ap peculiarities (Ap SrCrEu, Ap Si), and four emission-line stars were obtained using the MuSiCoS échelle spectropolarimeter attached the 2 m Bernard Lyot telescope at l'Observatoire du Pic du Midi, during four runs between Feb. 1997 and March 2000.

The MuSiCoS spectropolarimeter consists of an échelle spectrograph (Baudrand & Böhm 1992) and a dedicated polarimeter module (Donati et al. 1999) developed in the context of the MuSiCoS international collaboration. The spectrograph is a table-top instrument, fed by a double optical fibre directly from the Cassegrain-mounted polarization analyzer. In one single exposure, this apparatus allows the acquisition of a stellar spectrum in a given polarization state (in this case Stokes  $V$ ) throughout the spectral range 450 to 660 nm with a resolving power of about 35 000.

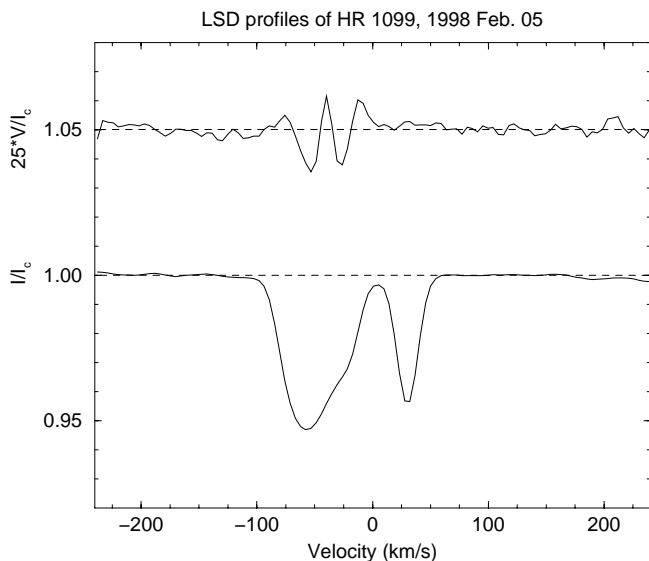


**Fig. 1.** LSD Stokes  $I$  (bottom) and  $V$  (top) profiles of the active RS CVn binary HR 1099. A strong ( $\sim 0.1\%$  amplitude) Stokes  $V$  signature (indicative of the presence of a photospheric magnetic field) is clearly detected, associated with the more rapidly rotating component. Note that, for display purposes, the Stokes  $V$  profiles have been expanded by a factor of 25 and shifted upward by 1.05.

In normal operation, starlight entering the analyzer at the Cassegrain focus is retarded by a rotatable quarter-wave plate. The beam then intersects a Savart-type beamsplitter which separates the stellar light into two beams which are respectively polarized (linearly) along and perpendicular to the instrumental reference azimuth. The analyzed beams are focal reduced to an aperture of  $f/2.5$  for injection into the double  $50/60\ \mu\text{m}$  fibre, which transports the light to the spectrograph. Spectra in both orthogonal polarizations are recorded simultaneously by the  $1024 \times 1024$  pixel SITE CCD detector.

A complete Stokes  $V$  exposure consists of a sequence of four subexposures, between which the retarder is rotated by  $90^\circ$ . This has the effect of interchanging the fibres through which each beam respectively passes, and thereby switches the positions of the two orthogonal circularly polarized spectra on the CCD. With such an observing procedure, all spurious signals are suppressed down to a level of typically  $2 \times 10^{-5}$  rms (Donati et al. 1997, 1999; Wade et al. 2000b). The échelle polarization spectra were reduced and extracted using the ESPRIT reduction package (Donati et al. 1997), in the manner described by Wade et al. (2000b).

One of the areas of concern in the reduction process is the fringing found in our spectropolarimetric instruments. The LSD technique of using many lines to compute the average profile greatly reduces the effect of fringing in the final profile, since the fringes will add incoherently in the averaging computation. LSD profiles computed for stars with fewer lines will be more greatly affected by the fringing.

### 3.1. Survey candidates

Am and HgMn targets were selected primarily from the catalogue of Abt & Morrell (1995) according to several criteria.

They are relatively bright with  $v \sin i$  less than about  $60\ \text{km s}^{-1}$ . The choices of Am stars with early A to early F metallic-line spectral types and HgMn stars with late B spectral types allow us to test the applicability of the LSD technique to stellar spectra of varying line density. We have specifically included HD 29173, HD 27295, HD 112412 ( $\alpha^1$  CVn), HD 195479, and HD 214994 (*o* Peg) in our study. HD 112412 is an Am star which was reported to be probably magnetic by Babcock (1967). The Am stars HD 29173 and HD 195479A (the primary component of the spectroscopic binary HD 195479) are reported by Lanz & Mathys (1993) as "... likely to possess... a magnetic field of about the same strength (as that of *o* Peg)". Analysis of the Am star HD 214994 was reported by Mathys and Lanz (1990) to be compatible with a 2 kG magnetic field. Hubrig & Castelli (2001) include HD 27295 in a list of HgMn stars likely to possess a magnetic field.

Normal stars were selected to sample the main sequence over the range of spectral type from B3 to F9, with several giant stars from B6 to F5 as well as  $\eta$  Leo (A0Ib) and  $\alpha$  Per (F5Ib). The two  $\lambda$  Boo stars were observed as a test of the applicability of the LSD technique to detect fields in high  $v \sin i$  stars with low line density spectra. Stars classified as having magnetic spectral peculiarities, but in which no magnetic fields have ever been detected, were observed in an attempt to also increase our knowledge of field structures in the weak-field magnetic Ap stars. Known magnetic stars were observed in order to illustrate the applicability of the LSD technique to measuring magnetic fields, and to improve upon existing longitudinal field measurements.

The journal of the stellar observations is presented in Table 1.

We obtained multiple observations for several objects, the details of which may be seen in Table 1. HD 48915 (Sirius), HD 77350, HD 78362, HD 108642, HD 110951 were each observed twice, with observations a year apart. HD 48915 and HD 126661 were each observed twice in two years. HD 141795 was observed three times over a period of 12 days in 1998, while HD 73709, HD 87737, HD 110379, HD 116656, and HD 129174 were each observed twice in the same year, with observations anywhere from five to thirty-three days apart). These observations were obtained in order to search for any temporal variability (perhaps due to rotational modulation) of a magnetic signal.

### 3.2. LSD linemasks

LSD mean signatures were computed using the technique described in Donati et al. (1997). The linemasks employed were computed using line lists from the Vienna Atomic Line Database (VALD) (Kupka et al. 1999; Ryabchikova et al. 1998), with appropriate abundance tables, effective temperatures and surface gravities. The abundance analyses of Adelman et al. (1997) and Adelman (1996) were examined to provide abundance tables for the Am stars as a function of effective temperature. Two characteristic abundance tables for Am stars were used; one for the hot Am stars (9000 K–10000 K) and one for the cooler Am stars ( $T_{\text{eff}} \leq 8500$  K). The abundance tables reported by Adelman (1992) were used

**Table 1.** Journal of observations. Am spectral types are the metallic-line spectral types by Abt & Morrell (1995).  $T_{\text{eff}}$  and  $\log g$  are determined from Strömgren photometry. The projected rotation velocities in Col. 6 are measured here, except as noted by \* which are from Abt & Morrell (1995) and by ‡ which are from Uesugi & Fukuda (1982). The heliocentric radial velocities in Col. 7 are measured here and are  $\pm 1 \text{ km s}^{-1}$  except where noted. A second rotation or radial velocity corresponds to that of a secondary star. Radial velocities marked with † are estimated from LSD profiles. The peak  $S/N$  obtained in each échelle spectrum is listed in Col. 10. The notation 2× in Col. 12 indicates that two identical observations were made in succession.

HD number	Spectral Type	$m_V$	$T_{\text{eff}}$ (K)	$\log g$	$v \sin i$ ( $\text{km s}^{-1}$ )	$v_{\text{rad}}$ ( $\text{km s}^{-1}$ )	HJD 2 440 000+	Exp (s)	$S/N$	LSD mask	Notes
<b>Am stars</b>											
29173	A1m	6.7	9070	4.22	$14 \pm 1$	15	11198.355	1440	170	Am9.0	
48915	A1m;SB1	-1.5	9970	4.32	$16.2 \pm 0.6$	-4	10502.371 10864.322	120 240	1650 2090	Am10.0	Sirius 2×
60178	A2Vm	2.9	9000	4.25	$20 \pm 1$	2	11584.536	2400	1410	Am9.0	$\alpha$ Gem B
73709	F2III	7.7	8080	4.02	$21.9 \pm 0.5$	25	11586.450 11611.476	2400 2400	90 120	Am8.0	
78209	F3m	4.5	7690	4.25	$38 \pm 1$	3	10854.447	1440	620	Am7.5	15 UMa
78362	F3m;SB1	4.7	7390	4.17	$11.3 \pm 0.5$	-10	10858.601 11202.550	1440 1600	460 490	Am7.5	$\tau$ UMa
89021	A2IV	3.4	8980	3.67	$50 \pm 2$	10	11579.681	2400	910	Am9.0	$\lambda$ UMa
90277	F2m	4.7	7480	3.50	$36 \pm 2$	18	10854.474	1440	440	Am7.5	30 LMi
95418	A1V	2.3	9630	3.87	$45 \pm 1$	13	11577.692	2400	1460	Am9.5	$\beta$ UMa
95608	A3m	4.4	8840	4.11	$18.3 \pm 0.6$	-11	11192.561	1440	350	Am9.0	60 Leo
97633	A2V	3.3	9290	3.64	$23.5 \pm 1.0$	$8 \pm 2$	11580.611	2400	1000	Am9.0	$\theta$ Leo
108642	A7m;SB2	6.5	8100	4.11	$< 10, < 10$	$34, -69^\dagger$ $-15, +22^\dagger$	10851.636 11197.710	2400 2400	240 190	Am8.0	
108651	F2m	6.6	8100	4.36	$23 \pm 1$	5	11204.684	1600	100	Am8.0	
109485	A0IV	5.4	9430	3.72	$18.6 \pm 0.5$	5	11601.637	2400	410	Am9.5	23 Com
110380	F0V	3.6	7830	4.57	$27 \pm 1$	-22	11587.639	2400	540	Am7.5	$\gamma$ Vir B
110951	F2m;SB2	5.2	7290	3.85	$19 \pm 3, 80 \pm 10$	$+15^\dagger$	10856.595 11201.674	1440 1600	380 360	Am7.0	32 Vir
112412	F3m	5.6	7010	4.36	$18 \pm 3$		10859.724	1600	330	Am7.0	$\alpha^1$ CVn
116657	A1m	4.0	9760	4.04	$51^*$		11587.712	2400	210	Am8.5	$\zeta$ UMa B
125337	A2m;SB2	4.5	9560	3.90	$< 10$	$0^\dagger$	11603.675	2400	350	Am8.5	$\lambda$ Vir
126661	F1m	5.4	7840	3.74	$36 \pm 2$	-28	10856.680 11606.591	1440 2400	370 220	Am8.0	22 Boo
141675	F3m;SB1	5.9	7910	4.11	$33 \pm 2$	-3	10857.725	1440	250	Am7.5	
141795	A7m	3.7	8450	4.20	$33.5 \pm 0.5$	-11	10851.738 10861.723 10862.726	1200 1200 1200	590 650 580	Am8.5	$\epsilon$ Ser 2× 2×
159560	F0m;SB1	4.9	7460	4.15	$42 \pm 1$	$-23 \pm 2$	10859.695	1200	310	Am7.5	$\nu^2$ Dra
195479	F2m;SB1	6.2	8480	4.08	$18.0 \pm 0.6$	-44	10860.738	1440	110	Am8.5	
214994	A1III	4.8	9600	3.62	$< 10$	9	11193.291	1440	370	Am9.5	$\rho$ Peg
<b>Ap HgMn stars</b>											
27295	B9HgMn	5.5	11970	4.23	$< 10$	4	11202.347	1440	320	HgMn12	53 Tau
63975	B8HgMn	5.1	13470	3.30	$28 \pm 3$	32	11203.501	1600	250	HgMn13	$\zeta$ CMi
75333	B9HgMn	5.3	12320	3.76	$36 \pm 3$	$30 \pm 2$	11202.516	2400	310	HgMn12	14 Hya
77350	B9SrCrHg	5.5	10320	3.61	$19.0 \pm 0.3$	-15	11201.627 11602.601	2000 2400	250 340	HgMn10	$\nu$ Cnc
78316	B8MnHg	5.2	13700	3.76	$< 10$	61	11192.609	1440	260	HgMn14	$\kappa$ Cnc
106625	B8gMn	2.6	12070	3.34	$37 \pm 4$	-3	11578.678	2400	1000	HgMn12	$\gamma$ Crv
129174	B9HgMn	4.9	13060	3.94	$16.4 \pm 0.8$	-1	11193.712 11198.756	1440 1440	300 430	HgMn13	$\pi^1$ Boo
143807	A0pHg	5.0	10780	3.99	$< 10$	-23	11603.714	2400	370	HgMn11	$\iota$ CrB
144206	B9HgMn	4.7	12070	3.79	$10.5 \pm 0.5$	3	11203.732	1440	350	HgMn12	$\nu$ Her
145389	B9p:Mn	4.2	11090	4.01	$10.9 \pm 0.2$	-19	11601.712	2400	450	HgMn11	$\phi$ Her

**Table 1.** Continued. Journal of observations.

HD number	Spectral Type	$m_V$	$T_{\text{eff}}$ (K)	$\log g$	$v \sin i$ (km s <sup>-1</sup> )	$v_{\text{rad}}$ (km s <sup>-1</sup> )	HJD 2 440 000+	Exp. (s)	$S/N$	LSD mask	Notes
<b><math>\lambda</math> Boo stars</b>											
110411	A0	4.9	8830	4.36	140*		11192.642	1440	280	$\lambda$ Boo9	$\rho$ Vir
125162	A0p	4.2	8610	4.24	110*		11608.650	2400	680	$\lambda$ Boo9	$\lambda$ Boo
<b>Normal stars</b>											
20902	F5Ib	1.8	6520	2.10	20 <sup>‡</sup>	-1 <sup>†</sup>	11587.411	1600	1360	solar6.25Ib	$\alpha$ Per
24760	B0.5V	2.9	25700	3.75	155 <sup>‡</sup>		11194.306	1200	630	solar26	$\epsilon$ Per
41753	B3V	4.4	17180	3.76	40 <sup>‡</sup>		11612.380	2400	250	solar17	$\nu$ Ori
61421	F5IV-V	0.3	6570	4.02	< 10	-3	11604.416	480	500	solar6.5	$\alpha$ CMi,2 $\times$
82328	F6IV	3.2	6360	4.08	10.5 $\pm$ 0.5	12	11600.577	2400	940	solar6.5	$\theta$ UMa
87737	A0Ib	3.5	10470	2.18	15 $\pm$ 2	1	11579.623	2400	880	solar10Ib	$\eta$ Leo
							11612.748	2400	960		
95382	A5III	5.0	8180	3.98	71*	-3	11608.537	2400	460	solar8.0	59 Leo
98353	A2Va:	4.8	8620	4.24	50 <sup>‡</sup>		11586.488	2400	260	solar9.0	55 UMa
99028	F4IV	4.0	6670	3.82	17 $\pm$ 1	-12	11599.584	1440	510	solar6.5	$\kappa$ Leo
104321	A5V	4.6	8080	3.51	61*		11608.572	2400	500	solar8.0	$\pi$ Vir
110379	F0V	3.6	6810	4.36	35 $\pm$ 1	-16	11587.608	2400	570	solar7.0	$\gamma$ Vir A
							11600.620	2400	850		
114710	F9.5V	4.3	6080	4.38	< 10	2	11599.608	1440	530	solar6.0	$\beta$ Com
118216	F2IV	4.9	6540	3.46	16.4 $\pm$ 1.0	4	11599.633	1440	340	solar7.0	BH CVn, RS CVn $v$
123299	A0IIISiCr	3.6	9950	3.62	28 $\pm$ 2	12	11599.706	1440	700	solar10	$\alpha$ Dra
123999	F9IV	4.8	6220	3.99	14 $\pm$ 3, 12 $\pm$ 3	54, -36 <sup>†</sup>	11603.640	2400	340	solar6.0	12 Boo
124850	F6III	4.1	6130	3.86	33 $\pm$ 1	12	11602.647	2400	700	solar6.0	$\iota$ Vir
126660	F7V	4.1	6370	4.35	30 $\pm$ 3	-10 $\pm$ 2	11580.691	2400	760	solar6.0	$\theta$ Boo
128167	F2V	4.5	6680	4.44	10 $\pm$ 1	2	11600.694	2400	540	solar7.0	$\sigma$ Boo
144284	F8IV	4.0	6290	3.99	30 <sup>‡</sup>	17 <sup>†</sup>	11584.756	2400	670	solar6.0	$\theta$ Dra
147394	B5IV	3.9	14940	3.84	30 <sup>‡</sup>		11579.726	2400	640	solar15	$\tau$ Her
155763	B6III	3.2	12500	3.50	43 $\pm$ 2	-14 $\pm$ 2	11580.733	2400	930	solar12.5	$\zeta$ Dra
160762	B3IV	3.8	17730	3.74	10 <sup>‡</sup>	-23 <sup>†</sup>	11606.673	2400	360	solar16	$\iota$ Her
<b>Ap SrCrEu, Si stars</b>											
60179	A1VSrEu	1.6	10000	4.0*	19 $\pm$ 1	1	11612.445	1200	1380	Ap10	$\alpha$ Gem A
74521	A1pEuCr	5.6	11720	3.47	10*	25 <sup>†</sup>	11612.414	2400	370	Ap10	49 Cnc
108662	A0pSrCrEu	5.2	11000	4.21	10*	-2 <sup>†</sup>	11612.536	2400	430	Ap10	17 Com
108945	A2pSr	5.4	8590	3.89	65*		11612.571	2400	390	Ap9	21 Com
115735	A0VHewk.	5.2	10750	3.99	90*	10 $\pm$ 3	11600.658	2400	410	Ap10	21 CVn
116656	A1VpSrSi	2.3	9430	4.22	25*	24 <sup>†</sup> , -18 <sup>†</sup>	11578.717	2400	1460	Ap9	$\zeta$ UMa A
						-9 <sup>†</sup>	11587.679	2400	1160		
120198	B9pEuCr	5.7	10460	3.81	45*	0 <sup>†</sup>	11601.673	2400	210	Ap10	84 UMa
125248	A0pCrEu	5.8	10750	4.36	10*	-16 <sup>†</sup>	11599.671	1440	200	Ap11	CS Vir,2 $\times$
						-16 <sup>†</sup>	11612.680	1440	240		
140160	A0	5.3	9220	4.16	65*		11606.630	2400	180	Ap9	$\chi$ Ser
148112	B9pCr	4.6	9440	3.69	35*		11602.688	2400	370	Ap9	$\omega$ Her
148330	A2SiSr	5.7	9510	3.75	10.5 $\pm$ 0.5	-7	11599.730	1440	270	Ap9	
<b>Emission-line stars</b>											
103287	A0Ve	2.4	9330	3.87	165*		11580.647	2400	1430	solar9.0	$\gamma$ UMa
108844	A5 $\delta$ Del	5.4	7960	3.76	78*		11586.665	2400	360	Am8.0	74 UMa
109387	B6IIIpe	3.9	13920	1.76	230 <sup>‡</sup>		11608.610	2400	880		$\kappa$ Dra
163472	B2IV-V	5.8	20350	3.65	120 <sup>‡</sup>		11586.712	2400	170	solar20	

to provide average HgMn abundances as a function of effective temperature, since almost all of the HgMn stars observed in our survey have been studied by Adelman. Characteristic abundance tables for HgMn stars having effective temperatures of 10 000 K, 11 000 K, 12 000 K, 13 000 K and 14 000 K were taken from that work. A characteristic  $\lambda$  Boo type abundance

table was adopted from Stürenburg (1993). An Ap SrCrEu abundance table was created by increasing the abundance of metals to 10 $\times$  solar, except for chromium which was increased to 100 $\times$  solar. All other line atlases were computed with solar abundances which are the default for the VALD database. The linemask used for analysis of an individual observation is given

**Table 2.** Details of the LSD linemasks used in this paper. The temperature is given as the numerical portion of the linemask name, in thousands of degrees.

LSD Linemask	$\log g$	Number of lines	Abundance References
Am10.0	4.0	570	<b>All Am masks:</b>
Am9.5	4.0	754	Adelman et al. (1997),
Am9.0	4.0	1054	Adelman (1996)
Am8.5	4.0	1561	
Am8.0	4.0	2202	
Am7.5	4.0	2793	
Am7.0	4.0	3000	
HgMn14	4.0	390	<b>All HgMn masks:</b>
HgMn13	4.0	429	Adelman (1992)
HgMn12	4.0	267	
HgMn11	4.0	429	
HgMn10	4.0	390	
$\lambda$ Boo9	4.0	168	Stürenburg (1993)
solar26	4.0	214	<b>All solar masks:</b>
solar20	4.0	189	VALD solar
solar17	4.0	210	
solar16	4.0	187	
solar15	4.0	268	
solar12.5	3.5	360	
solar10	4.0	402	
solar10Ib	2.0	603	
solar9.0	4.0	768	
solar8.5	4.0	1076	
solar8.0	4.0	1525	
solar7.5	4.0	1967	
solar7.0	4.0	2084	
solar6.5	4.0	2834	
solar6.25Ib	2.0	3156	
solar6.0	4.0	3114	
Ap9	4.0	2996	<b>All Ap masks:</b>
Ap10	4.0	1957	metals 10 $\times$ solar,
Ap11	4.0	1585	Cr 100 $\times$ solar

in Table 1, where the prefix (Am, HgMn,  $\lambda$  Boo, solar, or Ap) denotes the abundance table used, the numerical portion indicates the effective temperature used in thousands of degrees, and the suffix Ib indicates that the surface gravity used was appropriate for a supergiant star.

VALD linelists were requested to include all lines in the MuSiCoS spectral range with depths greater than 5% of the continuum. Several linelists were then tested to ascertain the cut-off in line depth which optimizes the  $S/N$  of the LSD extracted profiles. Initially, it was assumed that including weak lines would serve to dilute the profiles, since the average would then be computed by including many extremely noisy lines. Using LSD linelists with cut-off depths of 5%, 10%, 20%, 30% and 40%, we extracted LSD Stokes  $V$  profiles for a number of the Am and HgMn stars. When compared, we found that the LSD Stokes  $V$  profiles did not differ greatly as the depth cut-off criterion was changed. Since the contribution of each line to the average line profile is weighted by line depth, the shape of the profiles examined were essentially determined by the strongest

lines. The noise outside the lines, however, did decrease as more, weaker lines were used to extract the average (i.e. the linelist was cut off at a smaller depth). In some cases, the noise reached a minimum when linelists cut-off at 10% were used, while for others, using lines down to 5% seemed to reduce the noise even farther. In order to remain consistent, in the final analysis all linelists were cut off to include lines deeper than 10% of the continuum.

In the cases where Landé factors,  $g$ , were available from VALD for spectral lines, they were adopted for linemasks. Otherwise, except for the case of neon, values of  $g$  were calculated in LS coupling from the quantum numbers  $S$  and  $L$  as determined from the term information corresponding to each transition as provided in the VALD linelists, and  $J$  given explicitly in the VALD linelists. Landé factors for neon energy levels, for which LS coupling is a poor approximation, were taken from Moore (1949) where available, and the rest were calculated in pair coupling according to Sigut (1999). While the departure from LS coupling may be important for some individual lines, we do not expect this to significantly degrade our linelists for LSD profile extraction. Most lines in our linelists have experimentally determined or calculated Landé factors in the VALD database, and the inclusion of hundreds of lines in each linelist diminishes the effect which departures from LS coupling in a few lines may have.

### 3.3. Stellar parameters

Stellar effective temperatures and surface gravities were determined primarily from Strömgren photometry compiled by Hauck & Mermilliod (1998) using the calibration of Moon & Dworetzky (1985) with the following exceptions. The parameters for the hot star HD 41753 were taken from analysis by Castelli (1991) which uses an extension of the Moon & Dworetzky (1985) grid. HD 60178 and HD 60179 ( $\alpha$  Gem A & B) did not have Strömgren photometry available individually, so estimates of their temperatures and surface gravities were taken from the analysis by Smith (1974). For the B6III star HD 155763, for which Strömgren photometry is unavailable, ( $T_{\text{eff}}$ ,  $\log g$ ) parameters were adopted from Adelman (1996).

Values of  $v \sin i$  and radial velocity were obtained where possible for stars in this study using the technique of comparison with synthesized spectral regions as outlined by Landstreet (1998). The details of the technique are found in that reference, and the spectrum synthesis code, ZEEMAN, is described by Landstreet (1988) and Landstreet et al. (1989). The code searches automatically for a synthesized spectrum which best fits the observed spectrum, by varying chemical abundance,  $v \sin i$  and radial velocity. The code was run using the values of  $T_{\text{eff}}$  and  $\log g$  given in Table 1, and at a constant microturbulent velocity,  $\xi$ . The code was rerun while varying  $\xi$ , and the resulting best-fit abundances were plotted versus  $\xi$  in Blackwell diagrams for different lines of the same chemical species, namely for the Fe II  $\lambda\lambda$  4620, 4625, 4629 and 4635 lines and also for the Cr II  $\lambda\lambda$  4616, 4618 and 4634 lines. In all cases for which  $v \sin i$  and radial velocity have been obtained, the variation of

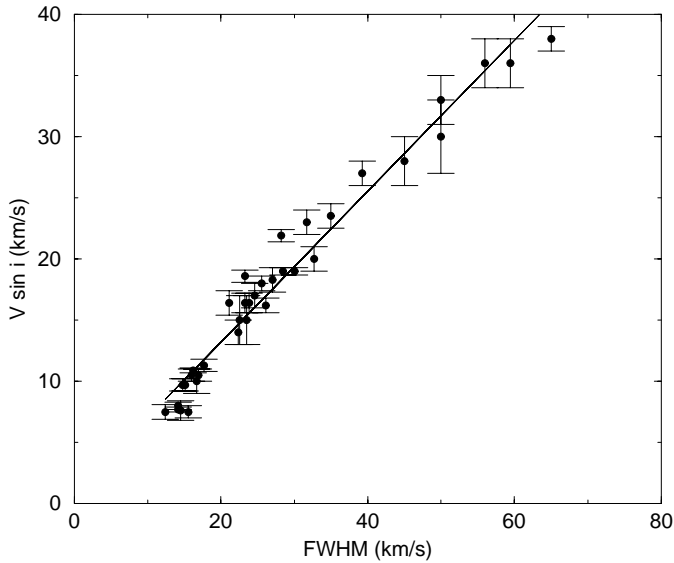


**Fig. 2.** Relationship between  $v \sin i$  as measured by spectral synthesis comparison and  $FWHM$  of gaussian fits to LSD Stokes  $I$  profiles for stars in this survey

determined abundance with microturbulent velocity for a given species converged at a common value of  $\xi$  and then values of  $v \sin i$  and radial velocity from the best-fit synthesized spectra at that value of  $\xi$  were averaged to provide us with the values given in Table 1.

Several stars have not had their rotation and radial velocities measured in this way, most often due to composite spectra or too high a  $v \sin i$ , and thus lines which are too broad for the small synthesis window used for the comparisons. The code was run without using its capabilities to include the effects of magnetic fields on the spectral lines, and thus it was impossible to use it to measure accurately the values pertaining to the sharpest-line magnetic Ap stars. In cases where stars had lines which could not be measured using the spectral synthesis comparison technique, radial velocities have been estimated from their position in LSD profiles. This is done mainly for spectroscopic binaries for which the primary was modelled by the synthesis code but the secondary was not.

Values of  $v \sin i$  have also been estimated from a few LSD profiles using an approximate linear relationship between stellar rotation velocities and the full-width at half-maximum ( $FWHM$ ) of gaussian fits to their LSD Stokes  $I$  profiles. This relationship is shown in Fig. 2 and the linear regression solution is

$$v \sin i = (0.617 \pm 0.020) \times FWHM + (0.86 \pm 0.61). \quad (1)$$

Using this relationship, we have obtained estimates of rotation velocities for several stars from their LSD profiles, as listed in Table 3. Uncertainties are estimated from the scatter of  $v \sin i$  about the regression relation.

#### 4. Results

No significant circular polarization was detected for any of the Am, HgMn,  $\lambda$  Boo, normal or emission-line stars. The criterion for detection of polarization is the statistical test described

**Table 3.** Estimates of  $v \sin i$  for some stars in this survey determined using the  $FWHM$  of gaussian fits to their LSD line profiles and Eq. (1).

Star	$v \sin i$ (km s <sup>-1</sup> )
HD 106625	37 ± 4
HD 108642 (secondary)	< 10
HD 110951	19 ± 3
HD 112412	18 ± 3
HD 123999 (primary)	14 ± 3
HD 123999 (secondary)	12 ± 3

by Donati et al. (1997) in which reduced  $\chi^2$  statistics are computed for the Stokes  $V$  profile inside and outside the spectral line. The statistics are then converted to detection probabilities (Donati 1992) and the probabilities are assessed to determine if significant polarization is detected.

While the detection or non-detection of significant circular polarization does provide an unambiguous diagnosis of a star's magnetic field, we have additionally computed mean longitudinal magnetic fields for the stars in our survey in order to make comparisons with previous measurements, and to provide a simple quantitative magnetic field diagnostic which may be analyzed statistically. The mean longitudinal field has been the standard diagnostic of magnetic fields in A and B type stars, and provides a measure of the disk-integrated line-of-sight component of the magnetic field, suitably weighted and integrated over the stellar disk (Mathys 1989). We realize that the non-detection of longitudinal fields does not preclude the existence of highly complex fields, or even simple fields observed at unfavorable phases, and thus stress that it is the detection or non-detection of significant circular polarization in LSD profiles which is the basis for our determination of a star having a magnetic field.

Mean longitudinal magnetic fields,  $B_l$ , for all observations (except HD 109387, cf. Sect. 4.6) have been calculated from LSD averaged Stokes  $V$  and  $I$  profiles in velocity units as

$$B_l = -2.14 \times 10^{11} \frac{\int vV(v)dv}{\lambda z c \int [I_c - I(v)]dv} \quad (2)$$

where  $\lambda$  and  $z$  are respectively the mean wavelength and Landé factor of all the lines used to compute the average profiles (Donati et al. 1997; Wade et al. 2000b). The limits of integration are chosen by visually determining the extent of the Stokes  $I$  average line profile. Uncertainties associated with the longitudinal field measurements are calculated by propagating the photon statistical error bars through the reduction of the spectra and the LSD averaging process, and then scaled in the manner described by Wade et al. (2000a).

Longitudinal fields and associated  $1\sigma$  uncertainties are given in Table 4 for the Am, HgMn, normal and emission-line stars, and in Table 5 for Ap SrCrEu and Ap Si stars. In cases where two identical observations were made successively of the same star (indicated by 2× in Col. 12 of Table 1), the longitudinal field was measured for both observations and then the average taken to appear in Tables 4 and 5. The median of the  $1\sigma$  uncertainties associated with the longitudinal field measurements of all non-magnetic stars is 22 G.

**Table 4.** Summary of derived longitudinal magnetic fields ( $\pm 1\sigma$ ) for the Am, HgMn, normal and emission-line stars.

HD number	$B_l \pm \sigma$ (G)	HD number	$B_l \pm \sigma$ (G)
<b>Am stars</b>			
29173	$28 \pm 32$	109485	$-26 \pm 31$
48915	$1 \pm 7$	110380	$21 \pm 16$
	$10 \pm 6$	110951	$-2 \pm 14$
60178	$24 \pm 10$		$8 \pm 16$
73709	$66 \pm 39$	112412	$-1 \pm 18$
	$-58 \pm 53$	116657	$37 \pm 67$
78209	$3 \pm 10$	125337	$20 \pm 23$
78362	$-5 \pm 5$	126661	$20 \pm 23$
	$-3 \pm 5$		$-41 \pm 35$
89021	$66 \pm 22$	141675	$42 \pm 26$
90277	$-9 \pm 20$	141795	$-7 \pm 15$
95418	$-4 \pm 15$		$-7 \pm 15$
95608	$-3 \pm 21$		$1 \pm 12$
97633	$9 \pm 12$	159560	$33 \pm 34$
108642	$-15 \pm 17$	195479	$15 \pm 53$
	$11 \pm 18$	214994	$-32 \pm 20$
108651	$-14 \pm 56$		
<b>HgMn stars</b>			
27295	$22 \pm 34$	106625	$-29 \pm 46$
63975	$100 \pm 110$	129174	$-12 \pm 39$
75333	$-120 \pm 100$		$-2 \pm 29$
77350	$6 \pm 35$	143807	$31 \pm 17$
	$17 \pm 36$	144206	$-24 \pm 49$
78316	$-37 \pm 26$	145389	$-7 \pm 16$
<b>Normal stars</b>			
20902	$1 \pm 2$	110379	$20 \pm 8$
24760	$130 \pm 140$		$-9 \pm 12$
41753	$120 \pm 420$	114710	$5 \pm 4$
61421	$2 \pm 5$	118216	$39 \pm 18$
82328	$0 \pm 4$	123299	$-29 \pm 30$
87737	$4 \pm 14$	124850	$3 \pm 5$
	$6 \pm 13$	126660	$-2 \pm 7$
95382	$-80 \pm 43$	128167	$8 \pm 13$
98353	$120 \pm 120$	144284	$3 \pm 8$
99028	$20 \pm 8$	147394	$33 \pm 87$
104321	$-93 \pm 53$	155763	$41 \pm 43$
		160762	$13 \pm 43$
<b>Emission-line stars</b>			
103287	$-140 \pm 120$	163472	$150 \pm 330$
108844	$66 \pm 52$		

#### 4.1. Am stars

No significant Zeeman circular polarization (according to the statistical test described by Donati et al. 1997) was detected for any of the observations of all 25 Am stars. Twenty-four observations imply longitudinal fields significant at less than  $1\sigma$ . For nine observations we infer longitudinal fields significant at greater than  $1\sigma$ , with one of those between  $2\sigma$  and  $3\sigma$ , and another at  $3\sigma$ . The  $3\sigma$  detection is not thought to be significant because we observe no coherent signal in the Stokes  $V$  profile (see Sect. 4.1.3).

The median of the  $1\sigma$  longitudinal field standard errors for the Am stars is 18 G. In comparison, typical longitudinal field

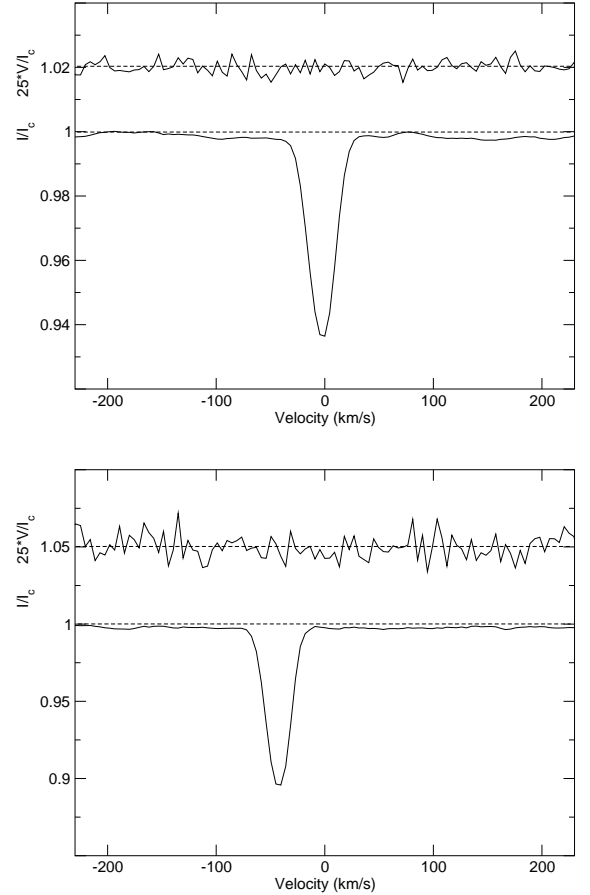


**Fig. 3.** LSD Stokes  $I$  and  $V$  profiles of the Am star HD 112412 (top) observed on HJD 2450859.724 and the Am SB1 HD 195479 (bottom) observed on HJD 2450860.738. In both cases the  $S/N$  is sufficient to rule out any signal with amplitude similar to that of HR 1099. Note that, for display purposes, the Stokes  $V$  profiles have been expanded by a factor of 25 and shifted upward by 1.02 (upper) and 1.05 (lower).

measurements previously obtained for Am stars (cf. Borra & Landstreet 1980; Landstreet 1982) were null detections with  $\sigma$ 's of 50 to 200 gauss. Our longitudinal field standard errors are all less than 50 G except for observations of the faintest stars ( $V_{\text{mag}} > 6$ ) and/or stars with relatively large rotation velocities ( $v \sin i > 50 \text{ km s}^{-1}$ ).

##### 4.1.1. HD 29173, HD 112412, HD 195479, HD 214994

We detect no circular polarization in the spectral lines of HD 29173, HD 112412, HD 195479A or HD 214994. stars for which magnetic fields have been reported using other methods. In Fig. 3 we show LSD Stokes  $I$  and  $V$  mean signatures for two of these stars. The  $S/N$  obtained for HD 112412 (330:1) is slightly lower than the median  $S/N$  (370:1) obtained for Am stars in this study, while that obtained for HD 195479 (110:1) is one of the lowest  $S/N$  obtained in this study. Nevertheless, the upper limits derived for these stars are considerably smaller than that required to detect a signal with amplitude comparable to that of HR 1099.



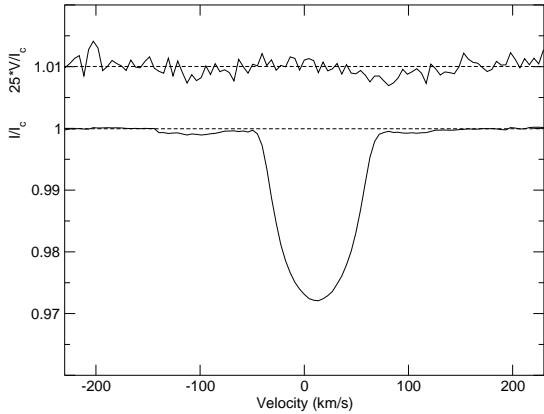


**Fig. 4.** LSD Stokes  $I$  and  $V$  profiles of the Am star HD 89021, observed on HJD 2451579.681. Although a longitudinal magnetic field is detected at the  $3\sigma$  level for this star, no significant polarization is seen in its Stokes  $V$  profile. Note that, for display purposes, the Stokes  $V$  profile has been expanded by a factor of 25 and shifted upward by 1.01.

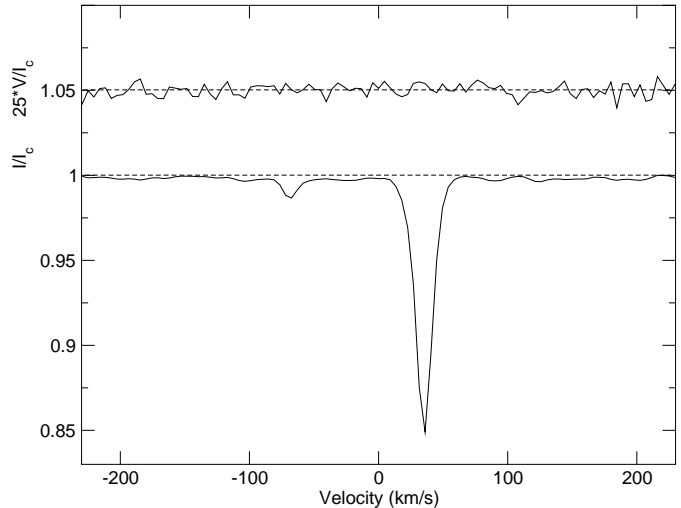


**Fig. 5.** LSD mean Stokes  $I$  and  $V$  profiles of the Am SB2 HD 108642, observed on HJD 2450851.636. The weak mean line of the secondary is clearly visible. Note that, for display purposes, the Stokes  $V$  profile has been expanded by a factor of 25 and shifted upward by 1.05.

#### 4.1.2. HD 48915 (Sirius)

Our observations of Sirius show no evidence for a magnetic field, and our two longitudinal field measurements are non-detections with  $\sigma = 6$  and  $7$  G. It is interesting to note that, while these standard errors are among the smallest we achieve in this study, similar precision has been achieved for Sirius using photoelectric polarimetric analysis of single lines by Borra et al. (1973), which gave null measurements of longitudinal field having  $\sigma$  as low as  $9$  G. Our observations do not confirm the measurements by Severny (1970) who reported a significant field of  $38$  G for Sirius.

#### 4.1.3. HD 89021

The measurement of the longitudinal field of HD 89021 is  $66 \pm 22$  G, which would seem to indicate a significant  $3\sigma$  detection. An examination of its LSD profiles, shown in Fig. 4, reveals no coherent signal in Stokes  $V$ , and we tentatively conclude that this measurement is spurious. We plan to re-observe this star in future in order to verify this conclusion.

#### 4.1.4. HD 108642

Two observations of HD 108642 (on HJD 2450851.636 and 2451197.710) show the mean line of the secondary in the unpolarized LSD profile. This object is well known as an SB1 and was discovered to be SB2 by Boesgaard (1987). The two observations of this system show a much weaker secondary mean line with approximately the same low rotation velocity (i.e.,  $<10$  km s $^{-1}$ ) as the primary (Fig. 5). Using the radial velocities of both components from both observations, we determine the systemic velocity to be  $V_0 = -2 \pm 2$  km s $^{-1}$ . Harper's (1929) orbital elements for this system include the systemic velocity  $V_0 = +1.78 \pm 0.37$  km s $^{-1}$ , which is consistent with our value. Using our measurements of the radial velocities of each component in each observation, we then compute the mass ratio,  $\mathcal{M}_1/\mathcal{M}_2 = 1.9 \pm 0.1$ . From the reason-

able assumption that the observed effective temperature and surface gravity ( $T_{\text{eff}} = 8100 \pm 300$  K and  $\log g = 4.1 \pm 0.3$ ; Landstreet 1998) correctly describe the primary, we find the mass of the primary  $\mathcal{M}_1 = 1.9 \pm 0.4 \mathcal{M}_\odot$  from its position on the  $\log T_{\text{eff}} - \log g$  diagram (using the theoretical evolutionary tracks for solar metallicity calculated by Schaller et al. 1992). This, in combination with the mass ratio, gives the secondary mass  $\mathcal{M}_2 = 1.0 \pm 0.2 \mathcal{M}_\odot$ . If we substitute for the masses in the mass function, using Harper's value of  $f(\mathcal{M}) = 0.0857$  we obtain the inclination of the orbital plane  $i \approx 64^\circ$ . This simple analysis therefore suggests that the secondary component of HD 108642 is a solar-mass dwarf, and the luminosity ratio  $L_1/L_2$  of the two components would be about 15. Therefore the flux of the primary does indeed dominate the system.

#### 4.1.5. HD 110951

We have detected the mean lines of both components of the SB2 HD 110951. This system is one in which the lines of the secondary indicate that it is hotter than the primary, implying evolution of the primary off the main sequence (Mitton & Stickland 1979). While detection of the lines of the secondary in this system had been reported previously (Mitton & Stickland 1979), its projected rotation velocity remained highly uncertain. Since this system is thought to contain a pulsating  $\delta$  Del star (the primary; Mitton & Stickland 1979), it is potentially very interesting for detailed study. From our first observation of HD 110951, shown in Fig. 6, we obtain for the secondary  $v \sin i = 80 \pm 10$  km s $^{-1}$  (where the error bar takes into account the uncertainty due to blending with the mean line of the primary), consistent neither with the results of Mitton & Stickland (1979) nor those of Kurtz et al. (1976) (who report  $v \sin i \sim 50$  km s $^{-1}$  and  $v \sin i = 140$  km s $^{-1}$  respectively). The  $v \sin i$  of the sharper-lined component is  $19 \pm 3$  km s $^{-1}$ , which is consistent with that obtained by Kurtz et al. 1976.

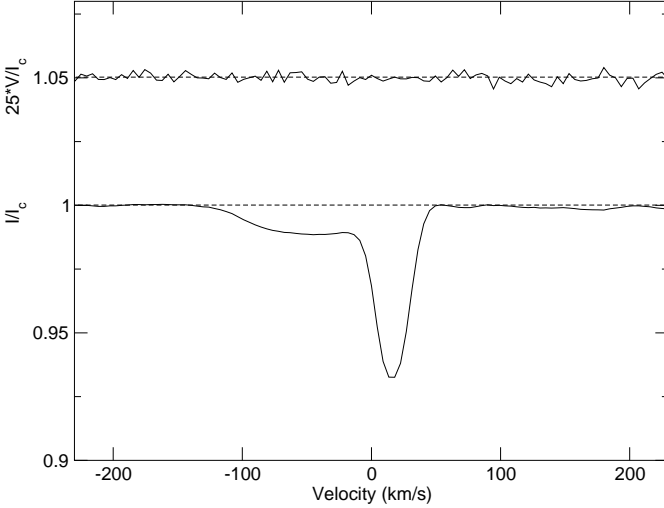


**Fig. 6.** LSD mean Stokes  $I$  and  $V$  profiles of the Am SB2 HD 110951, observed on HJD 2450856.595. Mean lines of both components are visible. Note that, for display purposes, the Stokes  $V$  profile has been expanded by a factor of 25 and shifted upward by 1.05.

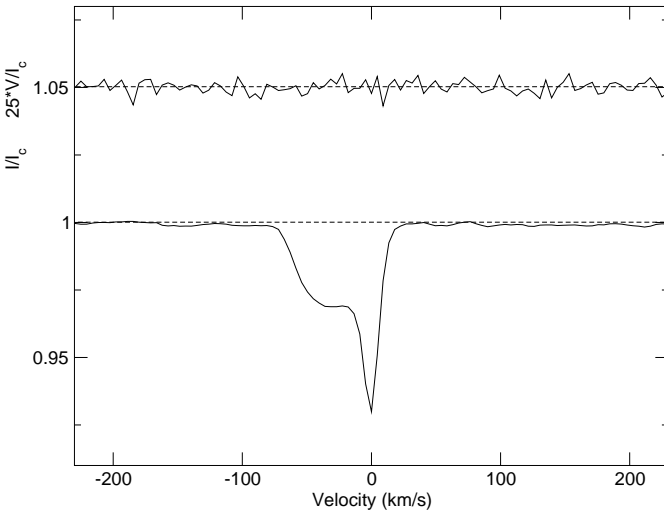


**Fig. 7.** LSD mean Stokes  $I$  and  $V$  profiles of the Am SB2 HD 125337, observed on HJD 2451603.675. The lines of both the sharp-lined component and broad-lined component are visible. Note that, for display purposes, the Stokes  $V$  profile has been expanded by a factor of 25 and shifted upward by 1.05.

#### 4.1.6. HD 125337

We have detected the lines of both components of the SB2 HD 125337 in its LSD line profile which is shown in Fig. 7. It is apparent that one star, believed to be the primary, is sharp-lined, and we estimate from the  $FWHM$  of its LSD profile that it has  $v \sin i < 10 \text{ km s}^{-1}$ , although with some uncertainty due to the difficulty in the fit of a gaussian to the broader lined component. We did not find it possible to accurately estimate the rotation velocity of the broad-lined component using our simple method, but its LSD profile is consistent with an approximate value of  $50 \text{ km s}^{-1}$ .

## 4.2. HgMn stars

No significant circular polarization is detected for any of the 12 observations of 10 HgMn stars. All 12 observations imply longitudinal fields significant at less than  $2\sigma$ , with nine significant at less than  $1\sigma$ . The median  $1\sigma$  longitudinal field standard error for the observations of HgMn stars is 39 G. Typical previous longitudinal field measurements of HgMn stars include those made by Borra & Landstreet (1980) which were non-detections with typical  $\sigma$ 's of 180 G.

### 4.2.1. HD 27295

No significant circular polarization is detected for HD 27295, although Hubrig & Castelli (2001) show evidence of magnetic intensification of Fe II lines for HD 27295, implying a possible magnetic field for this star. Chountonov (2001), used a “back-and-forth” magnetometry method and found its longitudinal field to be  $B_1 = +30 \pm 20 \text{ G}$ .

### 4.2.2. HD 78316 ( $\kappa$ Cnc)

No significant circular polarization is detected for HD 78316. The quadratic field of HD 78316 was measured by Hubrig (1998) to be  $2.7 \text{ kg}$ , significant at the  $6.3\sigma$  level. Hubrig (1998) also mentioned measurements of the longitudinal field of HD 78316 as being “...of the order of few hundred gauss at levels above  $3\sigma$ ” which would appear in a future, and as yet unpublished, paper. Since the diagnostics used to detect magnetic fields in HgMn stars have been primarily related to Fe II lines, we recomputed the LSD profiles for HD 78316 using only the Fe II lines in its spectrum. As expected, the resultant average profile was noisier (because fewer lines are used in the average, and lines other than Fe II, which may be blended in, are ignored) but still no significant circular polarization was observed. The corresponding longitudinal magnetic field measurement was  $B_1(\text{Fe}) = -24 \pm 41 \text{ G}$ , as compared to the measurement made using LSD profiles extracted from all spectral lines,  $B_1 = -37 \pm 26 \text{ G}$ .

Our longitudinal field measurement is also in contrast to the measurements made by Babcock (1958) and Preston et al. (1969), which seem to show periodic magnetic variability for HD 78316, with longitudinal fields ranging between  $+250$  and  $-150 \text{ G}$ , but with large uncertainties. Our non-detection is supported, however, by a non-detection made by Chountonov (2001) using a “back-and-forth” magnetometry method, which implied a longitudinal field of  $B_1 = +50 \pm 30 \text{ G}$ .

## 4.3. $\lambda$ Boo stars

The two  $\lambda$  Boo stars studied here, HD 110411 ( $\rho$  Vir) and HD 125162 ( $\lambda$  Boo) were studied by Bohlender & Landstreet (1990) using a  $H\beta$  Zeeman analyzer. Their measurements of the longitudinal fields resulted in non-detections with errors of around 200 G. Our measurements do not provide any detections of magnetic fields, but our errors are much larger ( $\sigma = 500 \text{ G}$  for HD 110411 and  $\sigma = 900 \text{ G}$  for HD 125162). Stars with the  $\lambda$  Boo chemical peculiarity are a good example of those

which are not suitable for analysis with the LSD technique. The low chemical abundance, with the resulting low line density, as well as the high projected rotation velocities typical of this class of star, mean that the multiplex advantage of averaging all the lines in a spectrum is greatly reduced. It should be noted that many O and early B-type stars may also be poor candidates for analysis with the LSD technique for the same reasons as for the  $\lambda$  Boo stars.

#### 4.4. Normal stars

No significant circular polarization is detected for any of the 24 observations of 22 normal (i.e. non-chemically peculiar, non-emission-line) stars. All 24 observations imply longitudinal fields significant at less than  $3\sigma$ , with 20 significant at less than  $2\sigma$ , and 17 significant at less than  $1\sigma$ . The median  $1\sigma$  longitudinal field standard error for the normal stars is 13 G. Previous longitudinal field measurements by Landstreet (1982) of some normal stars on our list also show no evidence for magnetic fields but have standard errors of  $\sigma$  ranging from 40 to 300 Gauss (300 G for one observation of HD 160762, a B3IV star).

##### 4.4.1. HD 20902 ( $\alpha$ Per)

HD 20902 is extremely well suited to the LSD technique, since it is quite bright, has a high line density due to its spectral type (F5Ib) and a moderately low projected rotation velocity of  $20 \text{ km s}^{-1}$ . We have measured its longitudinal fields to be  $B_1 = 1 \pm 2 \text{ G}$ . Borra & Landstreet (1973) did not detect a longitudinal field in this star, with  $\sigma = 60 \text{ G}$ .

##### 4.4.2. HD 61421 (Procyon)

We do not detect significant circular polarization for HD 61421. Our corresponding longitudinal field measurement of  $2 \pm 5 \text{ G}$  has one of the lowest errors in our survey, but it is not a large improvement over other measurements for this well-studied star. Landstreet (1982), using a coudé line profile scanner with polarization module, reported two non-detections with  $\sigma = 7 \text{ G}$ . Borra et al. (1984) made a longitudinal field measurement using circular spectropolarimetry of many lines simultaneously, in a technique resembling LSD, and found  $B_1 = -7.5 \pm 5.9 \text{ G}$ . Bedford et al. (1995), using a magneto-optical-filter spectrometer, made 12 measurements resulting in null detections with  $\sigma = 0.7\text{--}1.8 \text{ G}$ . Plachinda & Tarasova (1999) used a coudé spectropolarimeter along with their ‘‘Flip-Flop Zeeman Measurement’’ technique and measured the longitudinal field of HD 61421 to be  $B_1 = -1.34 \pm 1.0 \text{ G}$ .

##### 4.4.3. HD 98353

HD 98353 (55 UMa) has been classified as a  $\lambda$  Boo type star (Hauck 1986) but was later determined to be of spectral type A2 Va by Gray & Garrison (1987). It has also been classified as an A-shell star (Hauck & Jaschek 2000). Horn et al. (1996) suggest that it is the composite nature of the spectrum of this

**Table 5.** Longitudinal magnetic field measurements for the stars classified as Ap SrCrEu, Si.

HD number	HJD (2 440 000+)	$B_1 \pm \sigma(\text{G})$
<b>Ap SrCrEu,Si Stars</b>		
60179	11612.445	$26 \pm 13$
74521	11612.414	$634 \pm 17$
108662	11612.536	$-604 \pm 23$
108945	11612.571	$109 \pm 44$
115735	11600.658	$10 \pm 380$
116656	11587.679	$-9 \pm 16$
120198	11601.673	$-209 \pm 74$
125248	11599.671	$-10 \pm 43$
	11612.680	$-1496 \pm 43$
140160	11606.630	$230 \pm 120$
148112	11602.688	$-81 \pm 47$
148330	11599.730	$52 \pm 37$

triple system which has led to its being mis-classified, and that HD 98353 is not peculiar in any other way. Therefore, we have treated it as a normal star and do not find any significant circular polarization or evidence for a magnetic field in this star. The error in the longitudinal field measurement for this star, 120 G, is the largest for any A type star we have studied, except for the rapidly rotating emission-line star, HD 103287 and the  $\lambda$  Boo stars. We suspect it is the composite nature of the average line profile for HD 98353 which does not allow us to obtain a more precise result.

##### 4.4.4. HD 110379 ( $\gamma$ Vir A)

Babcock (1958) reported the field for HD 110379 to be  $B_1 = -390 \pm 50 \text{ G}$ . Boesgaard (1974) also detected a field for this star, varying between  $\sim -300 \text{ G}$  to  $\sim +400 \text{ G}$ , but with the variability seemingly unrelated to rotation. One measurement by Landstreet (1982) was a null with  $\sigma \approx 50 \text{ G}$ . Our two measurements of the longitudinal field of this star, separated by 13 days, both non-detections with  $\sigma \approx 10 \text{ G}$ , do not confirm the existence of a longitudinal field of several hundred gauss.

##### 4.4.5. HD 123999

HD 123999 is a known SB2, and our radial velocity measurements for the primary and secondary, given in Table 1, are in agreement with Fig. 3 of Boden et al. (2000).

#### 4.5. Ap SrCrEu stars

The 11 stars classified as Ap SrCrEu that were observed include five stars for which no fields have ever been detected, as well as six stars which are known to be magnetic. Of the stars previously not known to be magnetic, we have detected circular polarization in two; no significant polarization is detected for three others, with two observations implying longitudinal fields significant at less than  $1\sigma$  and one at  $2\sigma$ . The observations of the known magnetic stars show the expected circular polariza-

tion and corresponding longitudinal fields, except in the cases of HD 148112 and HD 148330, where we do not conclusively detect a magnetic field in one measurement of each star. The non-zero fields are listed in Table 5.

#### 4.5.1. HD 60179, HD 116656

Although HD 60179 and HD 116656 are classified as having the characteristic chemical peculiarities associated with magnetic fields, we detect no circular polarization in their spectral lines. A comparison of sections of their spectra to other, non-chemically peculiar, stars we have observed does not show the marked difference in the strengths of spectral lines of elements which one expects for the Ap SrCrEu type stars. For example, we do not observe markedly strong chromium lines for any either of these stars, and found Cr lines to be of similar strength to the Cr lines of Sirius. While this is not conclusive evidence that these stars are misclassified as magnetic peculiars, it suggests that misclassification is likely, especially since neither of these stars is identified as having variable photometry or line strengths (Catalano & Renson 1984 and supplements).

A measurement of the longitudinal field of HD 116656 on HJD 2451578.717 (our first observation) was not performed because of the blending of the line of the secondary with that of the primary, but no significant circular polarization was detected for that observation.

#### 4.5.2. HD 74521

The longitudinal field of this magnetic Ap star has been measured in the past with  $\sigma = 100\text{--}300$  G (Mathys 1991; Bohlender et al. 1993) and, as mentioned by Mathys (1991), “the variability of (the longitudinal field) in HD 74521 is far from being indisputably established.” There is also some uncertainty concerning the period of variation of HD 74521, if any such variation exists. Our single longitudinal field measurement of HD 74521, while very precise, is nearly at the mean of the previous field measurements and does little to confirm any variation.

#### 4.5.3. HD 108662

The longitudinal field of HD 108662 was previously studied by Babcock (1958), Preston et al. (1969) and Rustamov & Khotnyanskii (1980). It shows field variations between approximately +200 to  $-800$  G. Our single longitudinal field measurement,  $B_1 = -604 \pm 23$  G, is much more precise than any previous, and is in reasonable agreement with the observed field variation of previous measurements, when phased with the ephemeris of Rice & Wehlau (1994). More observations are necessary to improve the period.

#### 4.5.4. HD 108945

This is the first detection of circular polarization for the A2pSr star HD 108945 previously announced by Shorlin et al. (2001). Its LSD profiles are shown in Fig. 8, and clearly show a char-

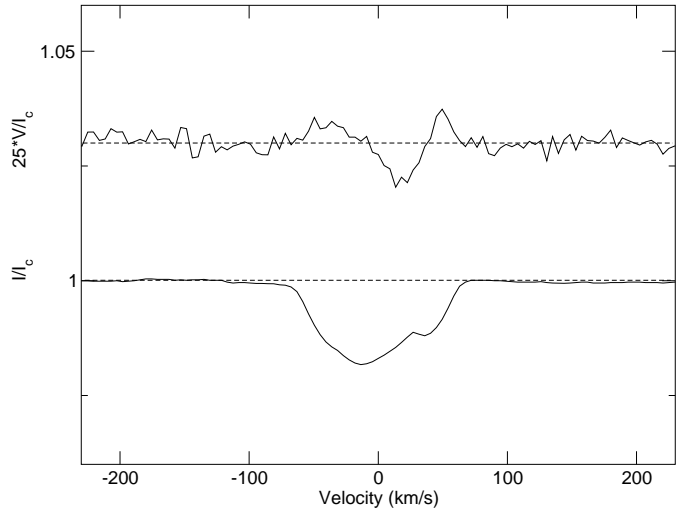


**Fig. 8.** LSD Stokes  $I$  and  $V$  profiles of the Ap Sr star HD 108945, observed on HJD 245162.571. A characteristic Stokes  $V$  profile for a magnetic Ap star may be seen. A “bump” in the Stokes  $I$  profile may also be seen, likely due to chemical abundance inhomogeneity on the stellar surface. Note that, for display purposes, the Stokes  $V$  profile has been expanded by a factor of 25 and shifted upward by 1.03.

acteristic Stokes  $V$  profile for a magnetic star which is definitely detected as determined by LSD (Donati et al. 1997). The asymmetry of the Stokes  $I$  profile is probably due to inhomogeneous chemical distributions on the stellar surface. Although our single longitudinal field measurement,  $B_1 = 109 \pm 44$  G, is significant at less than  $3\sigma$ , the detection of significant circular polarization in the Stokes  $V$  profile reveals this to be definitely a magnetic Ap star.

#### 4.5.5. HD 115735

HD 115735 has the highest rotation velocity of any of the classical magnetic Ap stars we observed, and while we do not detect significant circular polarization for it, it does not appear that it is misclassified or non-magnetic. Zverko (1984) shows that it is peculiar in that it has weak helium lines, although silicon does not seem to be of higher than normal abundance. Because of its high rotation velocity, HD 115735 is another example of a star which is not well-suited for our detection method.

#### 4.5.6. HD 120198

The longitudinal field of HD 120198 (84 UMa) has been measured by Borra & Landstreet (1980) and Wade et al. (1998), with typical standard errors of  $\approx 150$  G for the most recent observations. The variation evident in these measurements has allowed Wade et al. (1998) to determine the magnetic geometry for this star. Our single measurement,  $B_1 = -209 \pm 74$  G, when phased with the data of Wade et al. (1998) using their ephemeris, is in good agreement with the best-fit sinusoidal curve in their Fig. 1, and shows clearly that the field is variable.

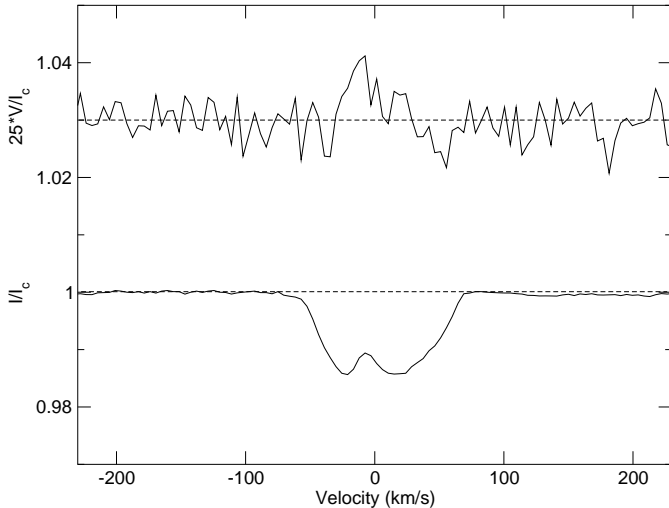


**Fig. 9.** LSD Stokes  $I$  and  $V$  profiles of the A0 SrCr star HD 140160, observed on HJD 2451606.630. Significant polarization is seen in the Stokes  $V$  profile. Note that, for display purposes, the Stokes  $V$  profile has been expanded by a factor of 25 and shifted upward by 1.05.

#### 4.5.7. HD 125248

HD 125248 (CS Vir) is an extremely well-studied magnetic Ap star, with many longitudinal field measurements made by authors from Babcock (1958) to Leone & Catanzaro (2001). Typical standard errors of previous longitudinal field measurements have been hundreds of Gauss, while we have made two measurements, both with  $\sigma = 43$  G. Our measurements are in nearly perfect agreement with the purely sinusoidal longitudinal field curve seen in Fig. 6 of Mathys & Hubrig (1997), when phased with their ephemeris. Our measurements are not in agreement, however, with the somewhat anharmonic best-fit longitudinal field curve in Fig. 10 of Leone & Catanzaro, when phased with their ephemeris. The curve of Leone & Catanzaro includes longitudinal field measurements made over the past fifty years from all available sources. Our data suggest that the longitudinal field of HD 125248 varies as described by Mathys & Hubrig.

#### 4.5.8. HD 140160

The longitudinal field of HD 140160 is not well-studied, with eight observations by Landstreet et al. (1975) and a single longitudinal field measurement by Borra & Landstreet (1980), none of which is significant at a  $3\sigma$  level. Leroy et al. (1993) observed HD 140160 using their broadband linear polarization method and found very low polarization. Our longitudinal field measurement,  $B_1 = 230 \pm 120$  G is significant at less than the  $2\sigma$  level, but the large amplitude of the circular polarization in the LSD Stokes  $V$  profile seen in Fig. 9 provides the first unambiguous detection of a magnetic field in this star. A signal is definitely detected as determined by LSD (Donati et al. 1997).

#### 4.5.9. HD 148112

HD 148112 ( $\omega$  Her) was observed by Borra & Landstreet (1980) and found to have a consistently negative longitudinal field, with some apparent variation between  $-570$  G and  $-15$  G, significant at less than  $2\sigma$ . Hatzes (1991) reported Doppler imaging of this star which shows inhomogeneities in the surface abundance of chromium, as is often seen in magnetic Ap stars. Our single observation does show a negative value of  $B_1 = -81 \pm 47$  significant at between 1 and  $2\sigma$ , but we do not conclusively detect a significant circular polarization signature.

#### 4.5.10. HD 148330

HD 148330 was found to be magnetic by Žižňovský & Romanyuk (1990), with a longitudinal field varying between  $-600$  and  $200$  G. We find no evidence for a magnetic field in our single observation of this star, but this is not inconsistent with the longitudinal field curve shown by Žižňovský & Romanyuk. When phased with their ephemeris, using a period of 4.288404 days, our longitudinal field measurement of  $B_1 = 52 \pm 37$  G is consistent with their near-zero longitudinal field measurements around phase 0.33. The non-detection of circular polarization in the LSD Stokes  $V$  profile is to be expected near polarity reversal for a star with low projected rotation velocity, when observed with only moderate  $S/N$ .

#### 4.5.11. Ap Star Summary

To summarize our data on Ap star: our field detections are consistent with previous measurements. All our non-detections are consistent with either (a) misclassification of what are likely not Ap stars, (b) observations at unfortunate phases or (c) very weak fields, of the order of the fields previously observed in the Ap star  $\epsilon$  UMa ( $B_1 \leq 100$  G, Wade et al. 2000b).

### 4.6. Emission-line stars

No significant circular polarization is detected in three emission-line stars, and the uncertainties in their inferred longitudinal fields are relatively large, due to high rotation velocities, relative faintness, and in the cases of the hottest examples, the relatively low number of lines in their spectra. Emission spikes in the spectrum of HD 109387 ( $\kappa$  Dra) made it impossible to extract LSD line profiles and thus to measure a longitudinal magnetic field.

## 5. Analysis

It is useful to examine the reasons why there is such wide range in longitudinal field uncertainty in this survey, with values varying from 2 G to hundreds of Gauss, or even  $10^3$  G if the  $\lambda$  Boo stars are considered. Assuming that the stellar magnetic fields are large-scale and produce a net longitudinal field, the uncertainty in a given longitudinal field measurement depends roughly on four values: the signal-to-noise ratio,  $S$ , of the spectrum, the number of lines,  $N$ , used to compute the average line

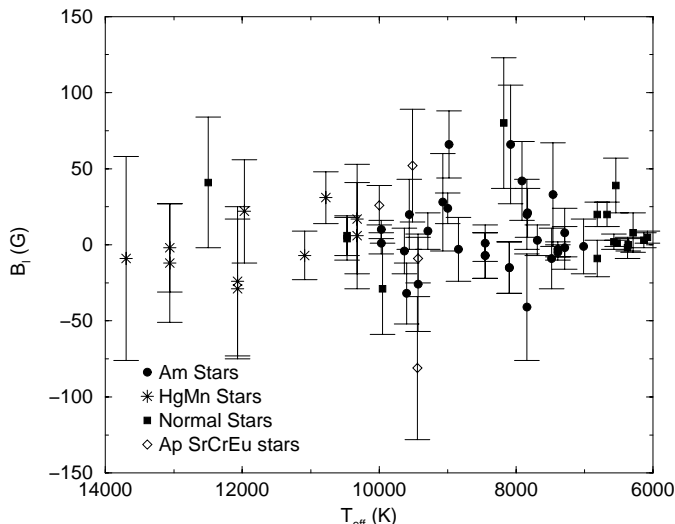


**Fig. 10.**  $B_1$  measurements of stars studied in this paper. In order to best visualize the most precise measurements, the nine with  $\sigma > 50$  G have been excluded from the figure. The other 64 are shown. Points corresponding to multiple measures of the same stars, or to stars with identical effective temperatures have been offset on the x-axis.

polarization profile, the depth,  $d$ , of the average line and the linewidth,  $\Delta\lambda$ , of the average line, in the following way:

$$\sigma \sim \frac{\Delta\lambda}{S d N^{1/2}} \quad (3)$$

or

$$\sigma \sim (v \sin i)^2 S^{-1} N^{-1/2} \quad (4)$$

since both  $\Delta\lambda$  and  $d^{-1}$  scale linearly with  $v \sin i$ . Aside from the variation of  $d$  with  $v \sin i$ , the *intrinsic* average line depth also affects the uncertainty in longitudinal field. Therefore, the very best candidates for field detection and measurement using this technique are stars with low  $v \sin i$  and many intrinsically strong lines. The LSD technique provides less precise results for stars with intrinsically weak lines, high  $v \sin i$  and/or few lines. This simple relationship explains the success of the LSD technique in measuring longitudinal fields in slowly rotating F, A and late B stars, especially those with chemical peculiarities which increase both intrinsic line depth as well as the number of lines found in their spectra. It also explains the relative failure of the LSD technique for the  $\lambda$  Boo and early B stars and other relatively fast rotators which have fewer lines in their spectra.

The measured values of  $B_1$  with  $1\sigma$  error-bars are plotted against stellar effective temperature in Fig. 10 in order to illustrate the very low standard errors achieved by using this method to measure fields, as well as the relative levels of success along the mid to upper main sequence. This figure includes only stars with  $\sigma < 50$  G, since those stars with larger uncertainties are the ones with high rotation velocities, fewer lines or lowest  $S/N$ , and are examples of stars for which our technique is not well-suited.

A histogram of the values of  $z = |B_1|/\sigma$  is shown in Fig. 11, compared to a normal distribution. It may be seen that in no longitudinal field measurement is the  $3\sigma$  level exceeded, and

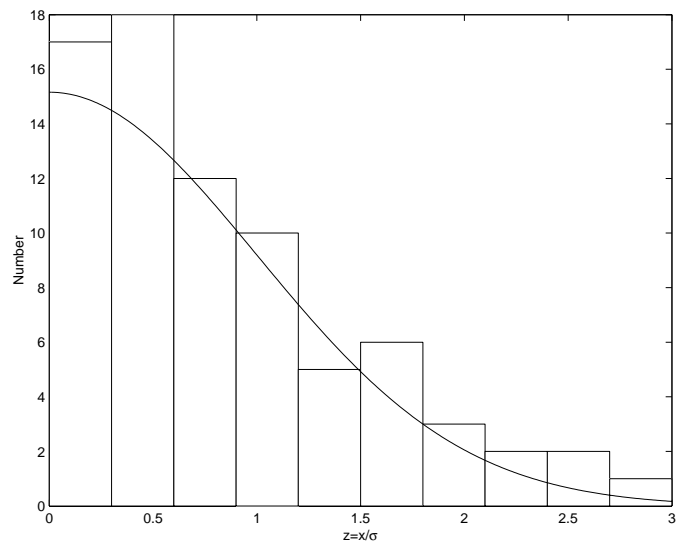


**Fig. 11.** Histogram of  $z = x/\sigma$ , where  $x = |B_1|$ , compared with a normal distribution.

that the distribution is somewhat over-concentrated towards zero. A truly normal distribution would exceed the  $1\sigma$  level in one-third of the measurements. Since the  $1\sigma$  level is exceeded in only approximately one-quarter of the measurements, this is an indication that perhaps the error-bars computed by LSD are a slight overestimate of the true uncertainty.

The distributions of the values of  $|B_1| + 1\sigma$  and  $|B_1| + 3\sigma$  for stars with  $\sigma < 50$  G is shown in Fig. 12. This distribution allows us to define envelopes of the upper limits on longitudinal field measurements for the stars best-suited to our method. These envelopes should be good indicators of the upper limits on longitudinal fields of the entire population of Am, HgMn and normal F, A and late B type stars. The  $1\sigma$  envelope in Fig. 12 allows us, with 67% confidence, to rule out for this population the existence of any longitudinal field larger than 90 G, and to say that at least half of the population will have longitudinal fields less than 40 G. The  $3\sigma$  envelope defines an extreme upper limit on longitudinal fields for this population. Even at the  $3\sigma$  confidence level (99.7%), at least half the stars have fields less than 70 G. It is instructive to contrast these values with longitudinal fields as large as 5 kG observed in some Ap stars (Mathys 1991; Hill et al. 1998) and a median of around 300 G (Bohlender & Landstreet 1990).

Assuming that the stellar magnetic fields are *not* large-scale in nature, i.e. more like those in cool active stars, the chances of detecting circular polarization signatures in LSD profiles is *increased* for stars with larger  $v \sin i$ , up to  $v \sin i \approx 50 \text{ km s}^{-1}$ . Light originating from regions of opposite magnetic polarity will be increasingly Doppler separated by increased rotation velocity, thus decreasing the amount of cancellation in the overall Stokes  $V$  profile, which will make it easier to detect. Since we do not detect polarization signatures in any Am, HgMn, and normal stars, including the fastest rotators, we conclude that they do not have fields similar to those of cool active stars. This conclusion is supported by the lack of secondary indicators of magnetic activity such as flares, spots, etc.

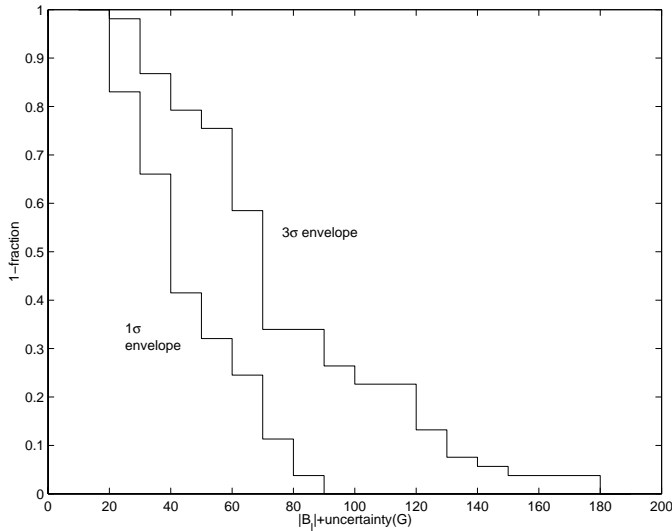


**Fig. 12.** Distribution of the absolute value of longitudinal field measurements plus  $1\sigma$  and  $3\sigma$  for stars with  $\sigma < 50$  G.

The observations presented in this paper therefore do not support the general existence of strong, complex magnetic fields, with topologies similar to, or simpler than, those observed in active late-type stars, in the photospheres of Am or HgMn stars. Since the existence of *ordered* fields is also ruled out by these and earlier observations (cited in Sect. 1), we conclude that the Am and HgMn stars in general do not display magnetic fields currently detectable by means which investigate circular polarization. There have been suggestions that toroidal fields may exist in these stars and that perhaps such fields would escape detection by circular polarization methods, but we *do* expect to be able to observe circular polarization for general geometries of toroidal fields in a rotating star using the LSD technique, due to the Doppler separation of the components of the Stokes  $V$  profile originating from the approaching and receding limbs of the star. In fact, toroidal field topologies in cool, active stars have been detected and studied previously using the LSD technique (Donati et al. 1997).

This result leads us to conclude that either the magnetic fields detected in these objects have topologies still considerably more complex than those found in active late-type stars, or that the detections of magnetic fields in these stars are spurious. The first conclusion cannot be excluded, although it would invoke a new kind of astrophysical phenomenon (the existence of strong, high fractional average stellar magnetic fields which are highly complex topologically). This option should be entertained within the context of our current knowledge of the kinds of magnetic fields which exist in stars: weak fields which are mildly topologically complex (in Sun-like stars and active late-type stars), and strong fields which are topologically simple (in the magnetic A and B type stars). The second conclusion is in principle also quite reasonable, since the reported field detections discussed in Sect. 1 are based upon measurements of the very subtle differential broadening of single pairs of spectral lines in the presence of a magnetic field, measurements susceptible to systematic errors, especially due to uncertainties in atomic physics and line blending.

## 6. Summary

We have searched for magnetic fields in the photospheres of 22 normal B, A and F stars, four emission-line B and A stars, 25 Am stars, 10 HgMn stars, two  $\lambda$  Boo stars and 11 magnetic Ap stars using circular spectropolarimetry and Least-Squares Deconvolution, a technique shown to be effective for detecting complex fields in active late-type stars (Donati et al. 1997). In none of the Am or HgMn stars is Zeeman circular polarization detected, from which we conclude that any magnetic fields which generally exist in the photospheres of Am and HgMn stars must be considerably weaker, considerably more complex or of a different structure than those found in active late-type stars. Measurements of the longitudinal magnetic field from each of our polarization spectra also result in no significant detection for any of the stars in our sample, with a median  $1\sigma$  uncertainty of  $\pm 18$  G for Am stars and  $\pm 39$  G for HgMn stars. In particular, we detect no fields in the Am stars HD 29173, HD 112412, HD 195479A or HD 214994 or the HgMn star HD 27295, for which non-zero field measurements have been reported.

We also detect no significant circular polarization for any normal star, ranging in spectral type from B0.5 to F9, including dwarfs, subdwarfs, giants and supergiants. The longitudinal field measurements resulted in no significant detections with a median  $1\sigma$  uncertainty of  $\pm 13$  G. No significant circular polarization was detected for any of the emission-line stars, although the uncertainty for these objects is higher. The LSD method was unsuited for the investigation of the two  $\lambda$  Boo stars, as well as the B6IIIpe star,  $\kappa$  Dra.

For the 12 stars classified as magnetic Ap stars, we provide the first detection of a field for HD 108945, as well as a convincing detection for HD 140160. We do not conclusively detect any field in HD 148112 ( $\omega$  Her) or HD 148330, stars previously shown to be magnetic, although our non-detections are consistent with previous studies. All other stars previously shown to be magnetic are reconfirmed here, and precise longitudinal field measurements have been made. Other stars classified as Ap SrCrEu, but for which no fields have been previously detected, were observed, but we find no evidence for their having fields. We suggest a reinvestigation of their spectral classifications.

We have furthermore remeasured the lines of the secondary in the spectrum of HD 108642. From our two measurements of the radial velocity separation of the components, we derive approximate values of the primary and secondary mass ( $M_1 = 1.9 \pm 0.4 M_\odot$  and  $M_2 = 1.0 \pm 0.2 M_\odot$ , respectively), the luminosity ratio ( $L_1/L_2 \approx 15$ ), and the inclination of the orbital plane ( $i \approx 64^\circ$ ). As well, we obtain a value of the projected rotation velocity of the rapidly rotating secondary component of the SB2 HD 110951,  $v \sin i = 80 \pm 10 \text{ km s}^{-1}$ . This value is inconsistent with previously published determinations.

*Acknowledgements.* Based on data obtained at l’Observatoire du Pic du Midi (CNRS).

SLSS acknowledges graduate scholarship support from an Ontario Graduate Scholarship in Science and Technology (OGSST).

JDL acknowledges grant support from the Natural Sciences and Engineering Research Council of Canada (NSERC).

We thank an anonymous referee whose comments contributed to the improvement of the manuscript.

This work has made use of the Simbad database, operated at CDS, Strasbourg, France and the Vienna Atomic Line Database, operated at Institut für Astronomie, Vienna, Austria.

## References

- Abt, H. A., & Morrell, N. I. 1995, *ApJS*, 99, 135
- Adelman, S. J. 1992, *MNRAS*, 258, 167
- Adelman, S. J. 1996, *MNRAS*, 280, 130
- Adelman, S. J. 1998, *MNRAS*, 296, 856
- Adelman, S. J., Caliskan, H., Kocer, D., & Bolcal, C. 1997, *MNRAS*, 288, 470
- Babcock, H. W. 1958, *ApJS*, 3, 141
- Babcock, H. W. 1967, in *The Magnetic and Related Stars*, ed. R. C. Cameron (Mono Book Corporation, Baltimore)
- Baudrand, J., & Böhm, T. 1992, *A&A*, 259, 711
- Bedford, D. K., Chaplin, W. J., Davies, A. R., et al. *A&A*, 1995, 293, 377
- Bikmaev, I. F., Musaev, F. A., Galazutdinov, G., Savanov, I. S., & Savel'eva, Yu. Yu. 1998, *Astron. Rep.*, 75, N1
- Boden, A. F., Creech-Eakman, M. J., & Queloz, D. 2000, *ApJ*, 536, 880
- Boesgaard, A. M. 1974, *ApJ*, 188, 568
- Boesgaard, A. M. 1987, *ApJ*, 321, 967
- Bohlender, D. A., & Landstreet, J. D. 1990, *MNRAS*, 247, 606
- Bohlender, D. A., Landstreet, J. D., & Thompson, I. B. 1993, *A&A*, 269, 355
- Borra, E. F., Edwards, G., & Mayor, M. 1984, *ApJ*, 284, 211
- Borra, E. F., & Landstreet, J. D. 1973, *ApJ*, 185, 139L
- Borra, E. F., & Landstreet, J. D. 1980, *ApJS*, 42, 421
- Borra, E. F., Landstreet, J. D., & Vaughan, A. H. 1973, *ApJ*, 185, 145L
- Borra, E. F., Landstreet, J. D., & Thompson, I. B. 1983, *ApJS*, 53, 151
- Castelli, F. 1991, *A&A*, 251, 106
- Catalano, F. A., & Renson, P. 1984, *A&AS*, 55, 371
- Chountonov, G. 2001, in *Magnetic Fields Across the H-R Diagram*, ed. G. Mathys, S. Solanki, & D. Wickramasinghe, *ASP Conf. Ser.*, 248, 385
- Conti, P. S. 1969, *ApJ*, 156, 661
- Donati, J.-F. 1999, *MNRAS*, 302, 457
- Donati, J.-F., Semel, M., & Rees, D. E. 1992, *A&A*, 265, 669
- Donati, J.-F., & Collier Cameron, A. 1997, *MNRAS*, 291, 1
- Donati, J.-F., Semel, M., Carter, B. D., Rees, D. E., & Collier Cameron, A. 1997, *MNRAS*, 291, 658
- Donati, J.-F., Catala, C., Wade, G. A., et al. 1999, *A&AS*, 134, 149
- Gray, R. O., & Garrison, R. F. 1987 *ApJS*, 65, 581
- Harper, W. E. 1929, *Pub. DAO*, 3, 315
- Hatzes, A. P. 1991, *MNRAS*, 253, 89
- Hauck, B. 1986, *A&A*, 154, 349
- Hauck, B., & Jaschek, C. 2000, *A&A*, 354, 157
- Hauck, B., & Mermilliod, M. 1998, *A&AS*, 129, 431
- Hill, G. M., Bohlender, D. A., Landstreet, J. D., et al. 1998, *MNRAS*, 297, 236
- Horn, J., Kubát, J., Harmanec, P., et al. 1996, *A&A*, 309, 521
- Hubrig, S. 1998, *Contributions of the Astronomical Observatory Skalnaté Pleso*, 27, 296
- Hubrig, S., & Castelli, F. 2001, *A&A*, 375, 963
- Kupka, F., Piskunov, N. E., Ryabchikova, T. A., Stempels, H. C., & Weiss, W. W. 1999, *A&AS*, 138, 119
- Kurtz, D. W., Breger, M., Evans, S. W., & Sandmann, W. H. 1976, *ApJ*, 207, 181
- Landstreet, J. D. 1982, *ApJ*, 258, 639
- Landstreet, J. D. 1988, *ApJ*, 326, 967
- Landstreet, J. D. 1998, *A&A*, 338, 1041
- Landstreet, J. D., Borra, E. F., Angel, J. R. P., & Illing, R. M. E. 1975, *ApJ*, 201, 624
- Landstreet, J. D., Barker, P. K., Bohlender, D. A., & Jewison, M. S. 1989, *ApJ*, 344, 876
- Lanz, T., & Mathys, G. 1993, *A&A*, 280, 486
- Leone, F., & Catanzaro, G. 2001, *A&A*, 365, 118
- Leroy, J. L., Landolfi, M., & Landi Degl'Innocenti, E. 1993, *A&A*, 270, 335
- Mathys, G. 1988, in *Elemental Abundance Analyses (Inst. Astr. Univ. Lausanne, Chavennes-des-Bois)*, 82
- Mathys, G. 1989, *Fund. Cosmic Phys.* 13, 143
- Mathys, G. 1991, *A&AS*, 89, 121
- Mathys, G., & Hubrig, S. 1995, *A&A*, 293, 810
- Mathys, G., & Hubrig, S. 1997, *A&AS*, 124, 475
- Mathys, G., & Lanz, T. 1990, *A&A*, 230, L21
- Mitton, J., & Stickland, D. J. 1979, *MNRAS*, 186, 189
- Moon, T. T., & Dworetzky, M. M. 1985, *MNRAS*, 217, 305
- Moore, C. E. 1949, *Atomic Energy Levels*, Vol. 1 (NBS Circ. 467; Washington DC: GPO)
- Plachinda, S. I., & Tarasova, T. N. 1999, *ApJ*, 514, 402
- Preston, G. W. 1974, *ARAA*, 12, 257
- Preston, G. W., Stepien, K., & Wolff, S. C. 1969, *ApJ*, 156, 653
- Rao, S. S., Abhyankar, K. D., & Nagar, P. 1990, *ApJ*, 365, 336
- Rustamov, Yu. S., & Khotnyanskii, A. N. 1980, *SvAL*, 6, 202
- Ryabchikova, T. A., Piskunov, N. E., Stempels, H. C., Kupka, F., & Weiss, W. W. 1998, *Proc. of the 6th International Colloquium on Atomic Spectra and Oscillator Strengths*, Victoria BC, Canada, *Physica Scripta*, T83, 162
- Schaller, G., Schaerer, D., Meynet, G., & Maeder, A. 1992, *A&AS*, 96, 269
- Severny, A. 1970, *ApJ*, 159, 73L
- Shorlin, S. L. S., Landstreet, J. D., Sigut, T. A. A., et al. 2001, in *Magnetic Fields Across the H-R Diagram*, ed. G. Mathys, S. Solanki, & D. Wickramasinghe, *ASP Conf. Ser.*, 248, 423
- Sigut, T. A. A. 1999, *ApJ*, 519, 303
- Smith, M. G. 1974, *ApJ*, 189, 101
- Stürenburg, S. 1993, *A&A*, 277, 139
- Wade, G. A., Donati, J.-F., Landstreet, J. D., & Shorlin, S. L. S. 2000a, *MNRAS*, 313, 823
- Wade, G. A., Donati, J.-F., Landstreet, J. D., & Shorlin, S. L. S. 2000b, *MNRAS*, 313, 851
- Wade, G. A., Hill, G. M., Adelman, S. J., Manset, N., & Bastien, P. 1998, *A&A*, 335, 973
- Žižňovský, J., & Romanyuk, I. I. 1990, *BAICz*, 41, 118
- Zverko, J. 1984, *BAICz*, 35, 294